Biochimica et Biophysica Acta 1778 (2008) 2512–2519

Contents lists available at ScienceDirect

Biochimica et Biophysica Acta

journal homepage: www.elsevier.com/locate/bbamem

Amyloid-β peptide induces temporal membrane biphasic changes in astrocytes through cytosolic phospholipase A_2

Jacob B. Hicks [a], Yinzhi Lai [a], Wenwen Sheng [b], Xiaoguang Yang [a], Donghui Zhu [a], Grace Y. Sun [c], James C-M. Lee [a,*]

[a] Department of Biological Engineering, University of Missouri, Columbia, Missouri 65211, USA
[b] Department of Pathology and Anatomical Sciences, University of Missouri, Columbia, Missouri 65211, USA
[c] Department of Biochemistry, University of Missouri, Columbia, Missouri 65211, USA

ARTICLE INFO

Article history:
Received 7 February 2008
Received in revised form 21 July 2008
Accepted 22 July 2008
Available online 7 August 2008

Keywords:
Phospholipase
Alzheimer
NADPH oxidase
Amyloid beta peptide
Astrocytes

ABSTRACT

Oligomeric amyloid-β peptide (Aβ) is known to induce cytotoxic effects and to damage cell functions in Alzheimer's disease. However, mechanisms underlying the effects of Aβ on cell membranes have yet to be fully elucidated. In this study, Aβ 1–42 ($A\beta_{42}$) was shown to cause a temporal biphasic change in membranes of astrocytic DITNC cells using fluorescence microscopy of Laurdan. $A\beta_{42}$ made astrocyte membranes became more molecularly-disordered within the first 30 min to 1 h, but gradually changed to more molecularly-ordered after 3 h. However, $A\beta_{42}$ caused artificial membranes of vesicles made of rat whole brain lipid extract to become more disordered only. The trend for more molecularly-ordered membranes in astrocytes induced by $A\beta_{42}$ was abrogated by either an NADPH oxidase inhibitor, apocynin, or an inhibitor of cytosolic phospholipase A_2 ($cPLA_2$), but not by an inhibitor of calcium-independent PLA_2 ($iPLA_2$). Apocynin also suppressed the increased production of superoxide anions (O_2^-) and phosphorylation of $cPLA_2$ induced by $A\beta_{42}$. In addition, hydrolyzed products of $cPLA_2$, arachidonic acid (AA), but not lysophosphatidylcholine (LPC) caused astrocyte membranes to become more molecularly-ordered. These results suggest (1) a direct interaction of $A\beta_{42}$ with cell membranes making them more molecularly-disordered, and (2) $A\beta_{42}$ also indirectly makes membranes become more molecularly-ordered by triggering the signaling pathway involving NADPH oxidase and $cPLA_2$ in astrocytes.

Published by Elsevier B.V.

1. Introduction

Increased production of amyloid-β peptides (Aβ) and their deposition as amyloid plaques in brains have been implicated in the pathogenesis of Alzheimer's disease (AD). In fact, the soluble oligomeric form of Aβ is cytotoxic to neurons and glial cells [1]. The cleavage of amyloid precursor protein by γ-secretase at the transmembrane domain demonstrated a hydrophobic property of the peptide at the carboxyl terminal and their ability to bind lipids [2]. Studies also demonstrated the ability of Aβ to perturb membrane and alter synaptic functions, such as calcium signaling, activity of enzyme, and lipid transport [3–6]. It has also been reported that the alteration of synaptosomal membrane fluidity induced by Aβ may underline impairment in memory and learning [7]. However, the mechanism underlying the effects of Aβ on cell membrane properties has yet to be elucidated. In this study, we demonstrate that phospholipase A_2 (PLA_2) is involved in the mechanism underlying the effects of $A\beta_{42}$ oligomers on cell membrane phase properties.

Phospholipases A_2 (PLA_2) are enzymes catalyzing the cleavage of fatty acids from the *sn*-2 position of phospholipids to produce free fatty acids and lysophospholipids [8,9]. PLA_2 are generally grouped into three major types, the Ca^{2+}-dependent group IV cytosolic PLA_2 ($cPLA_2$), the Ca^{2+}-independent group VI PLA_2 ($iPLA_2$) and the Ca^{2+}-dependent group II secretory PLA_2 ($sPLA_2$) [10]. PLA_2 not only plays a role in maintenance of cell membrane integrity, they are also critical in regulating the release of arachidonic acid (AA), a precursor for eicosanoids [10]. PLA_2 has been implicated in a number of neurodegenerative diseases including AD [11,12]. A marked elevation in $cPLA_2$ in the nucleus basalis and hippocampal regions of the AD brain has been observed [13–15]. Excessive PLA_2 activity disrupts membrane fluidity and alters composition and subsequently, activity of membrane-dependent proteins, such as Na–K–ATpase, beta2- and alpha2-adrenergic receptors, norepinephrine and serotonin uptake, and imipramine binding [16]. Our previous study demonstrated that $A\beta_{42}$ oligomers increase localization of phosphorylated $cPLA_2$ with mitochondria in astrocytes, and that activations of both $cPLA_2$ and $iPLA_2$ are the key steps in $A\beta_{42}$ oligomer-induced mitochondrial dysfunction in astrocytes [17]. Therefore, it is reasonable to hypothesize that oligomeric Aβ perturbs cell membrane properties not only through direct interaction with or insertion into cell membranes, but also through stimulating signaling pathways involving PLA_2.

* Corresponding author. 240 Ag Eng Bldg, 1406 E. Rollins St, Columbia, MO 65211, USA. Tel.: +1 573 884 3686; fax: +1 573 882 1115.
E-mail address: Leejam@missouri.edu (J.C.-M. Lee).

0005-2736/$ – see front matter. Published by Elsevier B.V.
doi:10.1016/j.bbamem.2008.07.027

In this study, we applied fluorescence microscopy of an environmentally sensitive probe, Laurdan, integrated into membranes of astrocytic DITNC cells, to characterize the changes in membrane molecular order induced by oligomeric $A\beta_{42}$. Inhibition studies demonstrated the involvement of NADPH oxidase and $cPLA_2$ in $A\beta_{42}$-induced membrane molecular order changes in DITNC cells.

2. Materials and methods

2.1. Materials

Dulbecco's modified Eagle medium (DMEM), F12 medium, Iscoves's modified Dulbecco's medium (IMDM), phosphate-buffered saline (PBS), Tris-buffered saline (TBS), trypsin-EDTA, streptomycin-penicillin, and fungizone were from Invitrogen (Gaithersburg, MD). Fetal bovine serum (FBS) was from US Bio-Technologies (Parkerford, PA). Methyl arachidonyl fluorophosphonate (MAFP) and (s)-bromoenol lactone (BEL) were from Cayman Chemical (Ann Arbor, MI). Rabbit polyclonal $cPLA_2$ and phosphorylated-$cPLA_2$ (Ser505) antibodies were from Cell Signaling Technology (Beverly, MA). 6-dodecanoyl-2-dimethylaminonaphthalene (Laurdan), and dihydroethidium (DHE) were from Invitrogen (Eugene, OR). Bovine serum albumin (BSA), poly-D-lysine, arachidonic acid (AA), lysophosphatidylcholine (LPC), phorbol myristate acetate (PMA) and apocynin (Apo) were from Sigma (St. Louis, MO). $A\beta_{1-42}$ ($A\beta_{42}$) and $A\beta_{42-1}$ peptides were purchased from American Peptide Company, Inc (Sunnyvale, CA).

2.2. Cell culture

Immortalized rat astrocytes (DITNC) were purchased from ATCC (Rockville, MD., USA). Cells were maintained at 37 °C in a CO_2 humidified incubator. DMEM culture medium supplemented with 10% of fetal bovine serum, 1% of penicillin/streptomycin (100 U/100 mg/ml) and 1% of fungizone (250 mg/ml) was fed to the cells every 48 h. When cells grew to confluency, they were subcultured to new flasks or dishes accordingly. In preparation for subculture, cells were washed twice with PBS and then incubated with 3 ml of 0.05% Trypsin-EDTA at 37 °C for 5 min. Culture medium was added to stop the trypsin-EDTA enzyme reaction and cells were then sedimented by centrifugation at 2000 rpm for 10 min. After discarding the supernatant, cells were resuspended in the same culture medium mentioned above and seeded to desired dishes or plates according to experiment condition at $3\times10^4/cm^2$ density. Experiments were performed when cells achieved approximately 70–80% confluency.

2.3. Preparation of oligomeric $A\beta_{42}$

$A\beta_{42}$ was obtained from American Peptides and its oligomeric form was prepared according to the protocol described by Dahlgren et al. (2002) [18]. Briefly, the peptide (1 mg) in powder form was dissolved in 200 μL of hexafluoro-2-propanol (HFIP) and the solution was aliquoted into Eppendorf tubes. Organic solvent was removed using a speed vacuum apparatus. The Aβ film left in the tube was resuspended in DMSO and further diluted in Ham's F12 medium to make a 100 μM solution. The solution was incubated at 4 °C for 24 h prior to use. As negative control, $A\beta_{42-1}$ (American Peptides) was processed similarly. Electrophoretic analysis of $A\beta_{42}$ indicated a similar profile with oligomers in the preparation as described by Dahlgren et al. (2002) [18].

2.4. Cell treatment

DITNC cells were grown on polylysine-coated glass coverslips to approximately 60% confluency. Before the addition of necessary reagents, cells were incubated with a serum-free medium containing DMEM overnight. Cells with/without pretreatment of inhibitors (e.g. MAFP, BEL and apocynin in DMSO) for 1 h were treated with the desired concentration of stimulators (e.g. oligomeric $A\beta_{42}$, and PMA in PBS; AA and LPC in EtOH) at 37 °C.

2.5. Preparation of laurdan-labeled vesicles made from rat whole brain lipid extract

Lipids in rat brains were extracted following the procedure described by Zhang and Sun [19]. Briefly, brain tissue was homogenized in 10 ml of PBS and 40 ml of chloroform-methanol (2:1 v/v) was added. The mixture was centrifuged at 2000 g for 10 min. The lower organic phase containing the lipids was filtered through a Pasteur pipette column packed with glass wool and anhydrous Na_2SO_4. The lipid extract was collected and stored at −20 °C until use.

To prepare Laurdan-labeled vesicles, ~0.001 mol% of Laurdan was added to brain lipids dissolved in chloroform-methanol (2:1 v/v) solvent. The preparation of vesicles was accomplished by electroformation as described in Lee et al. (2001) [20].

2.6. Fluorescence microscopy of laurdan-labeled cells and visualization of membrane molecular order

A membrane environmentally sensitive probe, Laurdan, was applied to characterize phase properties (i.e., molecular order) of plasma membranes in cells. This compound has been applied to detect phase transitions of different lipid systems as well as natural membranes [21,22]. Based on the parameters introduced by Parasassi et al. [21,22], generalized polarization (GP) of Laurdan is defined as: $GP=(I_B-I_R)/(I_B+I_R)$, where I_B and I_R are the intensities at 440 nm and 490 nm respectively with a fixed excitation wavelength of 350 nm. A higher GP indicates a more molecularly-ordered membrane, and a lower GP indicates a more molecularly-disordered membrane. Also, it is believed that laurdan GP is the measure of the polarization or water partition at the membrane core near the headgroup interface, where the fluorescent moiety of Laurdan (i.e. the naphthalene group) should be located based on its chemical structure. However, the Laurdan GP should prove to reflect the overall local membrane order, as GP values have been found to be correlated well with the bending rigidity and transition temperature of various bilayer membranes from typical phospholipid vesicles to ultra-thick diblock copolymer membrane vesicles, suggesting that GP measurements for studying membrane order are not affected by membrane thickness [23]. In addition, it is important to be aware of the basic concept of Laurdan GP that Laurdan GP indicates defects in molecular packing of bilayer membranes which accommodate water molecules (i.e. water partition).

After treatment at 37 °C, cells attached on glass cover slips were washed twice with PBS and incubated with DMEM containing 1% Laurdan for 15 min. Excess Laurdan was removed by washing cells three times with PBS. The cover slips were then transferred to a Bioptechs FCS2 Focht live-cell thermal chamber (Butler, PA) filled with phenol red free DMEM medium, in which temperature was maintained at 37 °C. Laurdan has been proved to preferentially integrate into plasma membranes with this protocol [24].

Fluorescence microscopy of Laurdan labeled cells was accomplished with a Nikon TE2000-U inverted microscope with a 60×, NA 1.4 oil immersion objective lens. A dual view micro-imager was installed to the emission port of the microscope, which allowed the acquisition of a pair of fluorescent images from a sample simultaneously at the emission wavelengths of 446 and 499 nm with a 46 nm bandwidth. These pairs of fluorescent images were used to calculate the local GP values of the cells in the pixel basis. The local GP values were then used to reconstruct a GP-mapped image for direct visualization of local membrane phase properties in cells.

To compute spatially-distributed $GP(x,y)$ for constructing GP-mapped images by pseudo-color representation of $GP(x,y)$, paired

images obtained at emission wavelengths of 446 and 499 nm were processed as follows: (1) convolution of both images with a Gaussian kernel to reduce noise; (2) computation of the denominator by pixel-wise addition of both images; (3) obtaining thresholds of the result using Otsu's method to separate Laurdan-stained regions from the background; and (4) computation of GP(x,y) on a pixel-by-pixel basis with the additional condition that the resulting pixel is zero if the thresholded denominator is zero.

2.7. Measurement of superoxide anion production in astrocytes

Dihydroethidium (DHE) was used to determine superoxide anion (O_2^-) production following a modified protocol as described by Chapman et al. [25]. Upon contact with superoxide anions, oxoethidium, a highly fluorescent product from the oxidative reaction of DHE, binds to DNA, causing an increase in fluorescent intensity of the cell nuclei. In this study, DITNC cells were grown on 8-well chambers and serum starved overnight. Cells were rinsed twice with warm serum-free and phenol red-free (PR-Free) DMEM and incubated with DHE (5 μM) in PR-free DMEM at 37 °C for 30 min. After removing excess DHE, cells were suspended in PR-free DMEM containing $A\beta_{42}$, PMA, apocynin (Apo), Apo+$A\beta_{42}$, and Apo+PMA for 1 h prior to taken images.

Fluorescence microscopy for DHE was performed with a Nikon TE-2000 U fluorescence microscope and a 40×, NA 0.95 objective lens. Images were acquired using a cooled CCD camera controlled by a computer running a MetaVue imaging software (Universal Imaging, PA). The fluorescence excitation source was controlled with a Uni-Blitz mechanical shutter. For image acquisition, a short exposure time (100 ms) and low intensity excitation light were applied to minimize photo-bleaching. The fluorescent intensity of DHE in each cell was quantified by integrating the pixel-intensity of the cell. Background subtraction was done for each image prior to the quantification of DHE intensity of cells. Each experiment was repeated three times for statistical data analysis.

2.8. Western blot analysis

DITNC cells were cultured in 60-mm dishes until 90% confluent. After treatment as described above, cells were washed with ice-cold PBS twice and 200 μl cell lysate medium (62.5 mM Tris–HCl, pH 6.8, 2% w/v SDS, 10% glycerol, 50 mM dithiothreitol, 0.01% w/v bromophenol blue) were added. After collecting the cell lysate, protein concentrations were determined by the Bradford assay [26]. Equivalent amounts of protein for each sample were applied to 7.5% SDS-PAGE. After electrophoresis, proteins were transferred to nitrocellulose membranes (0.45 μm, Bio-Rad). Membranes were incubated in Tris-buffered saline, pH 7.4 with 0.5% Tween 20 (TBS-T) containing 5% non-fat milk for 1 h at room temperature. The blots were reacted with primary rabbit anti-cPLA$_2$ or anti-p-cPLA$_2$ or anti-lamin A/C (1:1000; Cell Signaling) at 4 °C overnight with gentle shaking. After washing with TBS-T, the membranes were incubated with goat anti-rabbit IgG-HRP (1:2000; Sigma) for 1 h at room temperature and then washed 3× with TBS-T. Proteins were detected and visualized by enhanced chemiluminescence using a SuperSignal West Pico Chemiluminescent Detection Kit (Pierce Biotechnology, Inc). cPLA$_2$ and p-cPLA$_2$ bands were detected at 105 kDa.

2.9. Statistical analysis

Data are presented as mean±SD from at least three independent experiments. Comparisons between groups were made with one-way ANOVA, followed by Bonferroni's post hoc tests. Comparison between two groups was made with paired t test. Values of $p<0.02$ are considered statistically significant.

3. Results

3.1. Oligomeric $A\beta_{42}$ induced temporal membrane biphasic changes in DITNC cells through NADPH oxidase

We applied the fluorescence microscopy of Laurdan integrated into plasma membranes of astrocytic DITNC cells to study the possible changes in membrane phase properties induced by oligomeric $A\beta_{42}$. Since Laurdan possesses both an electron donor and an electron receptor, fluorescent excitation can induce a large excited-state dipole. This strong dipole tends to locally align the surrounding molecules (e.g. water), which dissipates a small fraction of the excited state energy and produces a red shift in the emission spectrum. A molecularly-disordered membrane allows more water molecules to partition into the membrane core, which is manifested by a red shift of Laurdan's emission maximum [23,27]. To quantify this shift, Gratton and co-workers [27] have defined the generalized polarization (GP) which was applied to observe phase transitions of different lipid membranes [28,29] as well as cell membranes [24,30]. A higher GP value indicates a more molecularly-ordered membrane, while a lower GP value indicates a more molecularly-disordered membrane. It has also been proved that once it is integrated into the plasma membranes of astrocytes, it would be unlikely to diffuse further into the intracellular organelles due to the hydrophobic properties of Laurdan [24].

Pseudo-colored GP-mapped images were reconstructed for direct observation of changes in GP values at different time points in cells after treatment with 1 μM of oligomeric $A\beta_{42}$ (Fig. 1A). In our data analysis, we plotted GP–GP$_o$, where GP$_o$ is the GP of control experiment (i.e. no $A\beta_{42}$ treatment). Therefore, GP–GP$_o$ of the control is always zero, serving as a common reference datum. Fig. 1B shows that $A\beta_{42}$ oligomers made cell membranes become more molecularly-disordered within 30 min, as indicated by negative GP–GP$_o$ values. However, these GP–GP$_o$ values became more positive with time and was more molecularly-ordered compared to the control at 3 h after the oligomeric $A\beta_{42}$ treatment, as indicated by a positive GP–GP$_o$ value. In order to test whether oxidative stress induced by NADPH oxidase plays a role in the time-dependent changes in GP values, apocynin, was used to pretreat cells for 1 h followed by the treatment with oligomeric $A\beta_{42}$. Apocynin is an intracellular inhibitor of the NADPH oxidase assembly, and it inhibits the translocation of the cytosolic oxidase subunits p47-phox and p67-phox to the membrane fraction [31]. In the presence of apocynin, the GP–GP$_o$ values were negative, indicating more molecularly-disordered membranes (Fig. 1C). These results suggest that the activation of NADPH oxidase is required for oligomeric $A\beta_{42}$ to make DITNC cell membranes become more molecularly-ordered.

The treatment of $A\beta_{42}$ for cells not only affected the overall (macroscopic) changes in GP (i.e. GP–GP$_o$), but it also altered the distribution of GP. Fig. 1D (*upper*) shows GP ranging from −0.4 to 0.4 with a peak at GP≈−0.14. After treatment with $A\beta_{42}$ for 30 min, the population of high GP values was decreased, and the peak was found at GP≈−0.25 (Fig. 1D, *middle*). However, after treatment with $A\beta_{42}$ for 3 h, the population of high GP increased with two major peaks at GP=−0.06 and GP=0.1, which was suppressed by Apo (data not shown).

3.2. Oligomeric $A\beta_{42}$ caused artificial membranes made of rat brain lipid extract to become more molecularly-disordered

To rule out the factors of cellular processes contributing to $A\beta_{42}$-mediated changes in the molecular order of membranes, we examined changes in artificial membranes made of rat brain lipid extract. Fig. 2A showed that oligomeric $A\beta_{42}$ caused artificial membranes to become more molecularly-disordered, as indicated by negative GP–GP$_o$ values. For a negative control, we examined if the reversed

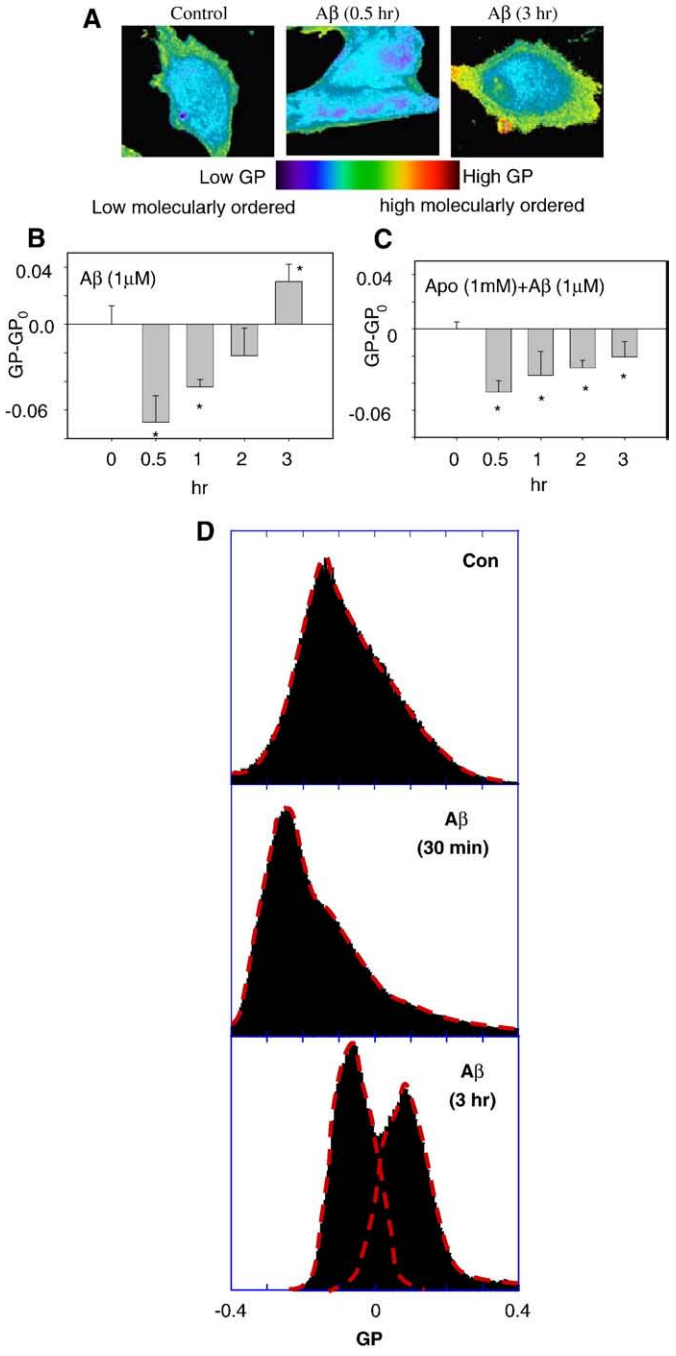

Fig. 1. $A\beta_{42}$ induced temporal biphasic changes of membrane molecular order in DITNC cells. (A) Pseudo-colored GP-mapped images of DITNC cells were reconstructed based on the GP value of each pixel. Control (*left*); a GP-mapped image taken at 0.5 h after treatment with 1 μM of $A\beta_{42}$ (*middle*); a GP-mapped image acquired at 3 h after treatment with 1 μM of $A\beta_{42}$ (*right*). (B) The GP–GP_o (GP_o = −0.0030 ± 0.016, is the GP of control sample without $A\beta_{42}$ treatment at time = 0) exhibited a negative value at 0.5 h after $A\beta_{42}$ treatment to cells, indicating more molecularly-disordered membranes, but a positive value at 3 h, indicating more molecularly-ordered membranes. (C) The GP–GP_o (GP_o = 0.074 ± 0.0051, is the GP of control sample treated with Apocynin (1 mM) in DMSO) exhibited only negative values in cells pretreated with apocynin (1 mM) for 1 h followed by $A\beta_{42}$ (1 μM) treatment. (D) Changes of GP distribution in response to the treatment of cells with $A\beta_{42}$; without treatment (*upper*); treatment with $A\beta_{42}$ for 30 min (*middle*); treatment with $A\beta_{42}$ for 3 h (*lower*).

amino acid sequence of Aβ (i.e. $A\beta_{42-1}$) affects the artificial bilayer membranes made of brain lipid extract. Fig. 2B shows that $A\beta_{42-1}$ only induced small changes in the molecular order of artificial membranes, and the changes were experimentally insignificant. These results are consistent with the notion that $A\beta_{42}$ directly interacts with membranes making them more molecularly disordered [32]. These results also lead to the hypothesis that $A\beta_{42}$ makes cell membranes become more molecularly-ordered through intracellular signaling pathways, which probably requires a long time (as shown in Fig. 1, it took more than 3 h for cell membranes to become more molecularly-ordered).

3.3. Oligomeric $A\beta_{42}$ increased superoxide anion production and phosphorylation of $cPLA_2$ through NADPH oxidase

To test the hypothesis that NADPH oxidase and $cPLA_2$ are involved in the $A\beta_{42}$-induced membrane biphasic changes in DITNC cells, we first examined whether oligomeric $A\beta_{42}$ increases superoxide anion (O_2^-) production and phosphorylation of $cPLA_2$ through

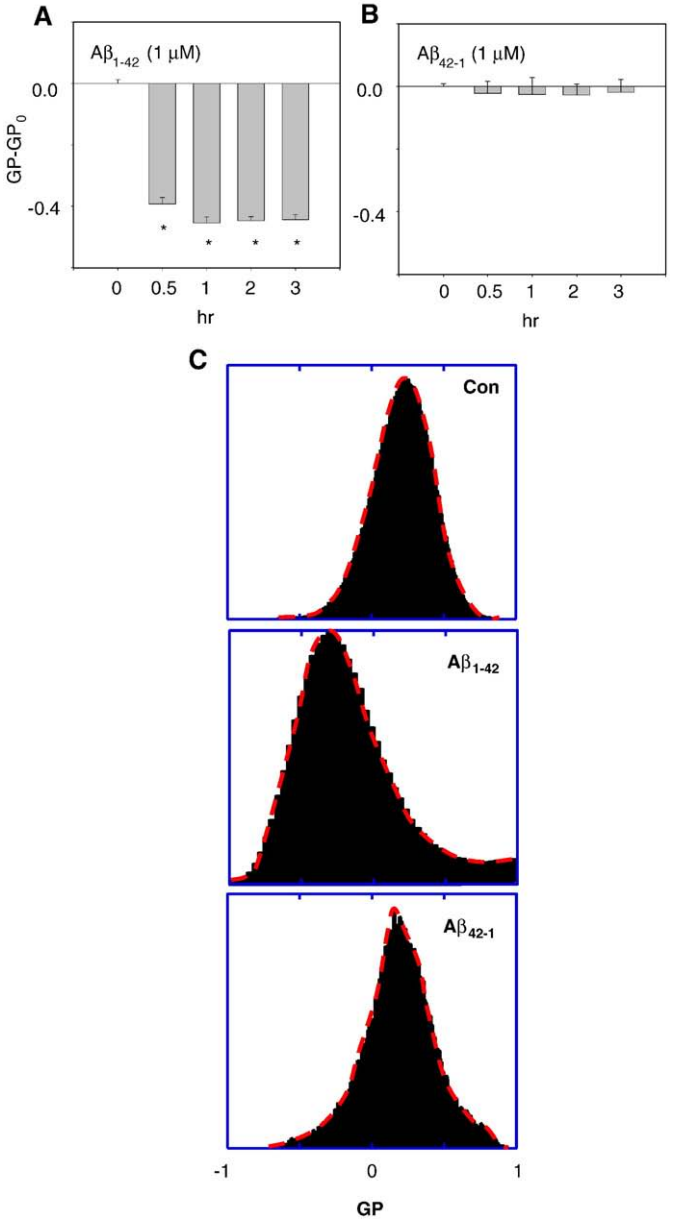

Fig. 2. $A\beta_{42}$ caused vesicle membranes of rat brain lipid extract to become more molecularly-disordered. (A) The GP–GP_o (GP_o = −0.24 ± 0.085, is the GP of control sample without treatment at time = 0) of Laurdan integrated in vesicle membranes of rat brain lipid extract after $A\beta_{42}$ treatment exhibited only negative values, indicating more molecularly-disordered membranes. (B) The reversed amino acid sequence of Aβ, $A\beta_{42-1}$, had no effect on the GP–GP_o value. (*$p < 0.02$) (C) The GP distribution after treatments with $A\beta_{1-42}$ and $A\beta_{42-1}$; without treatment (*upper*); treatment with $A\beta_{1-42}$ for 1 h (*middle*); treatment with $A\beta_{42-1}$ for 1 h (*lower*).

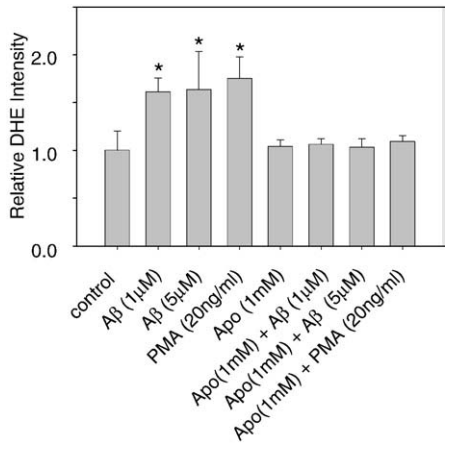

Fig. 3. $A\beta_{42}$ increased superoxide anion production through NADPH oxidase in DITNC cells. The fluorescent intensity of DHE was measured as an indicator of the superoxide anion (O_2^-) production level in cells. (*$p<0.02$) Apocynin suppressed the O_2^- production induced by $A\beta_{42}$, supporting that $A\beta_{42}$ increases O_2^- production in DITNC cells through NADPH oxidase.

NADPH oxidase in DITNC cells. We found that oligomeric $A\beta_{42}$ increased the production of O_2^- in DITNC cells, as indicated by increased fluorescent intensity of DHE. The increase of DHE intensity was suppressed by the inhibitor of NADPH oxidase, apocynin (Fig. 3). For a positive control, we treated cells with the phorbol ester (PMA), which has been reported to increase the production of superoxide anions in astrocytes through NADPH oxidase [33].

Western blot analysis of phosphorylated $cPLA_2$ (p-$cPLA_2$) shows that oligomeric $A\beta_{42}$ (1 μM) increased the immunoreactivity of p-$cPLA_2$ in DITNC cells, and this effect was suppressed by apocynin (Fig. 4). Since apocynin was dissolved in DMSO, DMSO alone was not able to trigger phosphorylation of $cPLA_2$. These results are consistent with our previous reported with primary astrocytes [17]. However, the response of DITNC cells to $A\beta_{42}$ treatment is slower as compared with that of primary astrocytes.

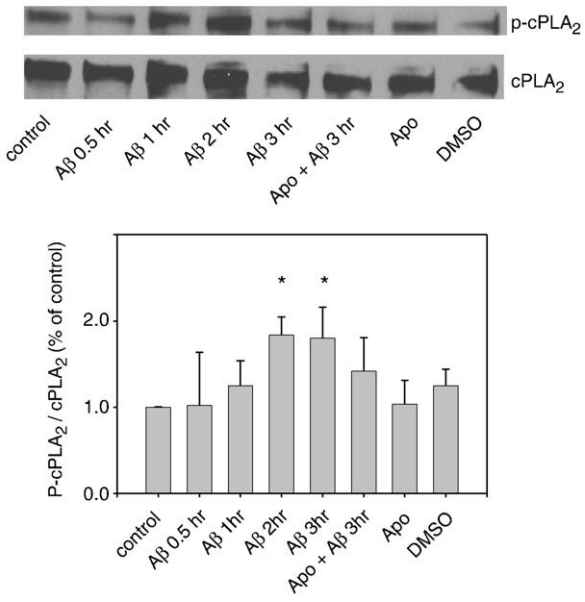

Fig. 4. $A\beta_{42}$ increased immunoreactivity of p-$cPLA_2$ in a time-dependent manner. DITNC cells were stimulated with $A\beta_{42}$ (1 μM) for different incubation times and were subjected to Western blot analysis with anti-p-cPLA2 and anti-$cPLA_2$ antibody. Results were from one representative experiment (*upper*). Repeated experiments gave similar results. For each sample, the relative intensity of phosphorylated $cPLA_2$ was normalized by the total $cPLA_2$ (*lower*). Values are the mean of three independent experiments. (*$p<0.02$)

3.4. $cPLA_2$ was the key enzyme involved in $A\beta_{42}$-induced membrane biphasic changes

Inhibitors of PLA_2 were applied to study the involvement of PLA_2 in $A\beta_{42}$-induced membrane changes in DITNC cells. When the inhibitor of $cPLA_2$ and calcium-independent PLA_2 ($iPLA_2$), methyl arachidonyl fluorophosphonate (MAFP), was added to cells and followed by treatment with $A\beta_{42}$, the GP–GP_o values only exhibited negative numbers (Fig. 5, *left*), indicating more molecularly-disordered membranes, and the ability of $A\beta_{42}$ to make membrane become more molecularly-ordered as indicated by a positive GP–GP_o value at 3 h in Fig. 1B was totally abrogated in Fig. 5, *left*. However, the specific inhibitor of $iPLA_2$, bromoenol lactone (BEL), was incapable of suppressing the membrane biphasic changes induced by oligomeric $A\beta_{42}$ (Fig. 5, *right*), which ruled out the role of $iPLA_2$. These results suggested that $cPLA_2$ (but not $iPLA_2$) was the key enzyme involved

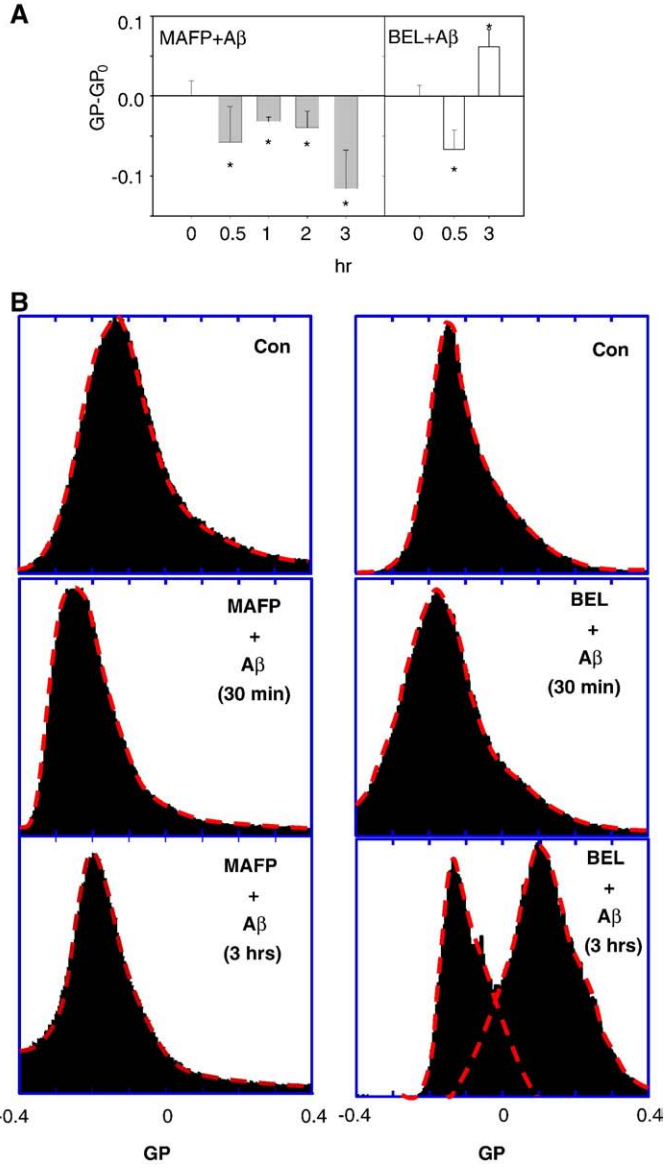

Fig. 5. Effects of PLA_2 inhibitors on $A\beta_{42}$-induced membrane changes in the molecular order. The membrane biphasic order changes induced by $A\beta_{42}$ (1 μM) was totally suppressed by MAFP (5 μM) as indicated by GP–GP_o values ($GP_o=0.074\pm0.06$, is the GP of control cells pretreated with 5 μM of MAFP in DMSO) exhibiting negative numbers only (*left*), but was not suppressed by BEL (5 μM) ($GP_o=-0.059\pm0.018$, is the GP of control cells pretreated with 5 μM of BEL in DMSO) (*right*). (B) GP distribution after treatment with $A\beta_{42}$ for cells pretreated with MAFP (*left*) and BEL (*right*).

in making membranes become more molecularly-ordered as observed in the biphasic changes of DITNC cell membranes induced by oligomeric $A\beta_{42}$.

The distribution of GP in Fig. 5B, (*lower right*) shows that BEL was incapable of suppressing the increased population of high GP domains with a peak at GP ≈ 0.1, whereas MAFP totally suppressed the formation of high GP domains (Fig. 5B, *lower left*). These results directly demonstrate that $A\beta_{42}$ makes membranes become more disordered, but also activates $cPLA_2$, resulting in the formation of high GP domains.

3.5. The hydrolyzed products of $cPLA_2$ made cell membranes become more molecularly-ordered

When $cPLA_2$ is activated, it targets and hydrolyzes phospholipids in cell membranes, resulting in hydrolyzed products, such as arachidonic acid (AA) and lysophosphatidylcholine (LPC). Since these hydrolyzed products of $cPLA_2$ may also contribute to the change of membrane molecular order induced by oligomeric $A\beta_{42}$ in DITNC cells, we applied the fluorescence microscopy of laurdan integrated in membranes of DITNC cells to study possible membrane changes caused by AA and LPC. We found that AA made membranes of DITNC cells more molecularly-ordered, as indicated by positive $GP\text{-}GP_o$ values; whereas LPC did not cause significant changes of membranes. Similarly, LPC did not cause any major effect on the GP distribution (Fig. 6, *right*). However, AA made significant changes in the distribution of GP (Fig. 6, *left*) and produced two major populations with their peaks at GP ≈ −0.1 and GP ≈ 0.025.

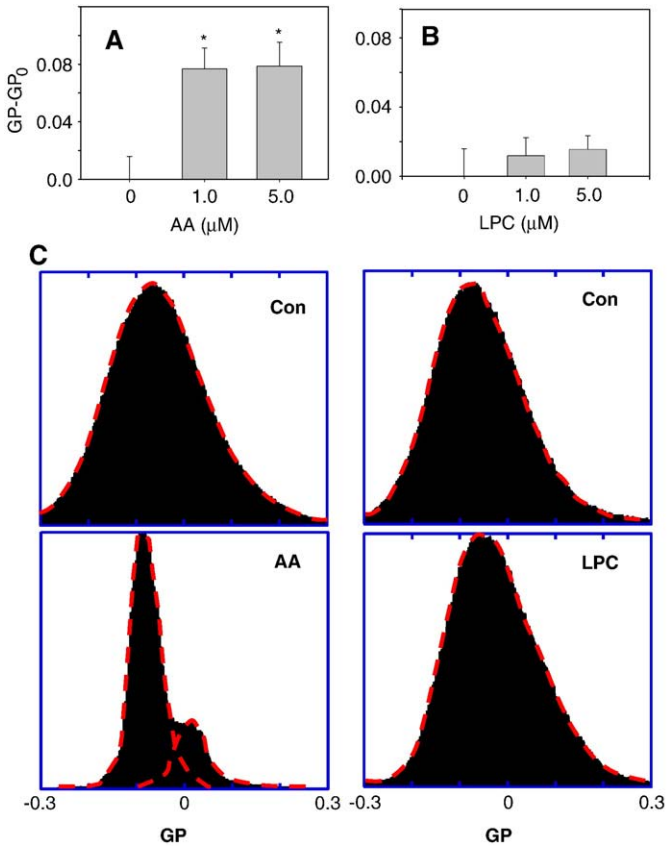

Fig. 6. Effects of hydrolyzed products of $cPLA_2$ on membranes in DITNC cells. (A) The treatment with arachidonic acid (AA) for 1 h caused cell membranes to become more molecularly-ordered, as indicated by positive $GP\text{–}GP_o$ values. (B) The treatment with lysophosphatidylcholine (LPC) for 1 h did not cause a significant change in GP. (*$p < 0.02$) ($GP_o = -0.038 \pm 0.016$ is the GP of control cells treated with ethanol, as both AA and LPC were dissolved in ethanol.) (C) GP distribution of DITNC cell membranes treated with AA (*left*) and LPC (*right*).

4. Discussion

Applying fluorescence microscopy of Laurdan integrated into membranes of astrocytic DITNC cells and artificial membranes made of rat brain lipid extract, we demonstrated that both NADPH oxidase and $cPLA_2$ were involved in the $A\beta_{42}$ oligomer-induced temporal biphasic membrane change in DITNC cells. Our data also suggest that a hydrolyzed product of $cPLA_2$, arachidonic acid (AA), contributes to the effect of $A\beta_{42}$ in causing cell membranes to become more molecularly-ordered through the activation of NADPH oxidase and $cPLA_2$.

The absolute changes of GP in artificial membranes made of whole brain lipid extract induced by $A\beta_{42}$ was about 0.4 (Fig. 2A), which was greater than that in $A\beta_{42}$-stimulated DITNC cells, where the maximum absolute change of GP can be estimated from the GP's at time points 0.5 h and 3 h to be about 0.1 (Fig. 1B). Fig. 1C also shows that the absolute change of GP in $A\beta_{42}$-stimulated cells pretreated with Apo to inhibit NADPH oxidase and $cPLA_2$ was about 0.04. Generally, the changes of GP in cells induced by $A\beta_{42}$ are smaller, as compared to those in artificial membranes, but they are statistically significant. In fact, the GP changes in DITNC cells measured here are comparable to the GP change (~0.13) in macrophages induced by removal of cholesterol with methyl β-cyclodextrin (mβCD) [34]. We observed that the GP's of controls (i.e. GP_o) did not change with time, but varied with different experiments, which is probably due to different inhibitors (e.g. Apo, MAFP, and BEL) being added to different controls, as these inhibitors contribute slightly to the emission at the wavelengths of 446 and 499 nm tested in PBS (data not shown).

In fact, a correlation between GP values and raft/non-raft domains has been established using liposomes with equal molar ratios of dioleoylphosphatidylcholine (DOPC), cholesterol, and sphingomyelin by Dietrich et al., 2001 [35]. Our GP distribution of artificial membranes made of whole brain lipid extract (Fig. 2C, *upper*) is comparable to that reported by Dietrich et al., 2001 [35]. GP > 0.55 and < −0.05 were found to represent membranes in gel and fluid phase, respectively. Moreover, (−0.05 < GP < 0.25) and (0.25 < GP < 0.55) represent membranes in liquid-disordered/nonraft domains and liquid-ordered/raft domains, respectively [35]. Separation of liquid-ordered and liquid-disordered phases has also been shown at GP values between 0.2 and 0.3 [36,37]. The GP values of cell membranes ranging from −0.4 to 0.4 reported here clearly provide evidence of a coexistence of both liquid-disordered/nonraft and liquid-ordered/raft domains. Interestingly, $A\beta_{42}$-induced $cPLA_2$ activation produced a major population of high GP domains with a peak at GP = 0.1 and a GP range of −0.1 to 0.4 (Fig. 1D, *lower*, and Fig. 5B, *right lower*). Since the GP of Lubrol-insoluble membranes at 37 °C has been reported to be 0.308 ± 0.126 [34], these results suggest that $A\beta_{42}$-induced cPLA activation in DITNC cells increases raft heterogeneity and phase separation in membranes. The distributions of GP (Fig. 1D, *lower*, and Fig. 5B, *right lower*) observed in $A\beta_{42}$-induced $cPLA_2$ activation are similar to those reported GP distribution in macrophage membranes at 37 °C [34]. Since macrophages are relatively active immune cells in which $cPLA_2$ can be frequently activated [38], we speculate that the GP distributions in macrophage membranes reported by Gaus et al., [34] might be affected in part by $cPLA_2$ activation.

In model membranes, areas of high curvature exhibit lower GP values than areas of low curvature [36]. However, for cell membranes similar differences in physical arrangement may not account for comparable changes in GP. It has been shown in living macrophages that variable surface morphologies, cell-to-cell contacts, and possible adhesion locations are enriched in high GP domains, and these high GP domains are likely a result of condensed membrane structure as opposed to differences in curvature [34]. In agreement with these results, our GP-mapped images of $A\beta_{42}$-stimulated DITNC cells (Fig. 1A) show an increase in high GP domains at cell edges, implicating local compositional changes, rather than differences in

curvature, as being responsible for the observed increase in high GP domains at these locations.

It is also important to note that PLA_2 exerts a unique effect on bilayer membranes. While PLA_2 causes membranes to become more molecularly-ordered as measured by Laurdan [39], surprisingly, it has also been reported that it causes membranes to become more fluidized [12,40–42]. More rigorously, Laurdan is a measure of defects in molecular packing of bilayer membranes which accommodate water molecules (i.e. water partition). Other membrane probes, such as 1,6-diphenyl-1,3,5-hexatriene (DPH), 1-(4-trimethylammoniumphenyl)-6-phenyl-1,3,5-hexatriene (TMA-DPH), and molecular rotor, (2-carboxy-2-cyanovinyl)-julolidine farnesyl ester (FCVJ), measure rotational motions of the probes, which reflects the size of free volume for diffusion. Therefore, the unique effect of PLA_2 on cell membranes suggests that lower water partitioning into membranes may not necessarily result in lower membrane fluidity. Clearly, more investigations are needed to examine the relationship between water partitioning into membranes and free volume in membranes. Since both $A\beta_{42}$ and PLA_2 cause membrane to become more fluidized, $A\beta_{42}$ does not produce a temporal biphasic change of membrane fluidity in DITNC cells (data not shown); therefore, fluidity study may not be able to probe the $cPLA_2$ pathway underlying the effect of $A\beta_{42}$ on membranes in DITNC cells.

The release of Aβ from its precursor protein (amyloid precursor protein) and its pathway leading to deposition of amyloid plaques have been regarded to play an important role in the etiology of AD [1,43]. Recent studies have demonstrated cytotoxic effects of Aβ, especially its aggregation to the oligomeric form [44]. These soluble diffusible protofibrils of Aβ have been shown to disrupt membranes, forming calcium channels [3] and causing increase in calcium influx [45] and triggering cell death pathways [3,45,46]. These properties of Aβ have induced interest in investigation of how Aβ aggregates impact on cell membrane properties.

Studies with synthetic membranes indicated the ability of oligomeric Aβ to perturb cholesterol containing membranes [2,47]. A number of studies indicated alteration of membrane fluidity by soluble Aβ [30,32,48–53]. In our study, we investigate cell membrane molecular order changes induced by oligomeric Aβ in DITNC cells, which allow us to address membrane changes not only due to the direct interaction of $A\beta_{42}$ oligomers with membranes, but also due to $A\beta_{42}$-triggered cellular processes.

Increase in oxidative stress has been regarded to play a role in the development of AD [54]. It has been reported that $A\beta_{42}$ increases the production of reactive oxygen species (ROS) in astrocytes through the superoxide producing enzyme, NADPH oxidase [17,55]. Oxidative stress has also been reported to trigger the MAPK pathways and subsequent activation of PLA_2 (Xu et al., 2002; Zhu et al., 2005). The relationship between $cPLA_2$ and NADPH oxidase under oxidative conditions has also been demonstrated in phagocytic cells [56–61]. In neutrophils, $cPLA_2$ was found in cytoplasm and plasma membranes, suggesting multiple role of this enzyme in regulating different subcellular membranes [62]. In this study, $A\beta_{42}$ oligomers activated NADPH oxidase and $cPLA_2$ in astrocytes, resulting in increased ROS production. In addition, this condition rendered astrocyte membranes to become more molecularly-ordered.

Immortalized rat astrocytes, DITNC cells, possess the phenotypic characteristics of type 1 astrocytes [63]. Similar to the finding with primary astrocytes [17], $A\beta_{42}$ induced ROS in DITNC cells and ROS production was inhibited by apocynin, a specific inhibitor for NADPH oxidase (Fig. 3). Aβ also increased phosphorylation of $cPLA_2$ in DITNC cells (Fig. 4). The ability for apocynin to inhibit Aβ-mediated $cPLA_2$ phosphorylation suggests a link between ROS and $cPLA_2$ activation through NADPH oxidase. However, it is interesting to note that DITNC cells respond to $A\beta_{42}$ stimulation much slower than primary astrocytes. While primary astrocytes took less than 15 min to activate $cPLA_2$ by $A\beta_{42}$ oligomers [17], DITNC cells took more than 1 h. The prolonged responsive time of DITNC cells provides an advantage allowing a longer time window for the examination of signaling pathways and measurement of cell membrane property changes. This unique feature provided advantage for using DITNC cell culture as a good cell model for study of astrocytes in neurodegenerative diseases.

Oligomers of $A\beta_{42}$, but not the monomeric peptide, has been reported to insert into cholesterol-containing phosphatidylcholine monolayers with an anomalously low molecular insertion area [2]. Consistent with the effect of $A\beta_{42}$ oligomers on artificial membranes made of rat brain lipids and membranes of DITNC cells within the first hour reported here, $A\beta_{42}$ oligomers have an enhanced disordering effect on membranes [32]. However, in membranes from brain lipids, $A\beta_{42}$ monomers render these artificial membranes to become more molecularly ordered [64]. $A\beta_{42}$ assembly at the bilayer surface is dependent on cholesterol, but does not result in bilayer disruption [64]. In our study, we observed a time-dependent transition of the DITNC membrane to become more molecularly-ordered upon incubation with Aβ oligomers. A similar time course for activation of $cPLA_2$ was observed (Fig. 4). Our results are consistent with study with erythrocytes in which secretory PLA_2 also renders these membranes to be more molecularly-ordered [39], and are consistent with the finding by others that arachidonic acid makes membranes become more molecularly-ordered [65].

Increasing evidence has been cumulated to suggest that oligomerization of amyloid peptides leads to alteration of cell membranes and cell signaling pathways. There are other examples in which protein misfolding is an important part of disease processes. For example, amylin, a molecule in Type II diabetes, also binds and disrupts membranes of insulin-producing β-cells [66]. There is further support that amylin can activate NADPH oxidase to increase ROS production in β-cells [67]. In the study here, we have demonstrated that NADPH oxidase and $cPLA_2$ are involved in the $A\beta_{42}$-oligomer-induced membrane biphasic change in astrocytic DITNC cells. Understanding the mechanism underlying cell membrane alterations induced by $A\beta_{42}$ should prove further our understanding in alteration of primary functions of membrane proteins and in the pathogenesis of AD.

Acknowledgments

This work was supported by NIH Grants 1P01 AG18357 and 1R21NS052385, Alzheimer Association Grant NIRG-06-25448, and MU Research Board Grant URB-04-038.

References

[1] D.J. Selkoe, Alzheimer's disease is a synaptic failure, Science 298 (2002) 789–791.
[2] R.H. Ashley, T.A. Harroun, T. Hauss, K.C. Breen, J.P. Bradshaw, Autoinsertion of soluble oligomers of Alzheimer's Abeta(1–42) peptide into cholesterol-containing membranes is accompanied by relocation of the sterol towards the bilayer surface, BMC Struct. Biol. 6 (2006) 21.
[3] N. Arispe, E. Rojas, H.B. Pollard, Alzheimer disease amyloid beta protein forms calcium channels in bilayer membranes: blockade by tromethamine and aluminum, Proc. Natl. Acad. Sci. U. S. A. 90 (1993) 567–571.
[4] H. Hartmann, A. Eckert, W.E. Muller, Apolipoprotein E and cholesterol affect neuronal calcium signalling: the possible relationship to beta-amyloid neurotoxicity, Biochem. Biophys. Res. Commun. 200 (1994) 1185–1192.
[5] J. McLaurin, A. Chakrabartty, Membrane disruption by Alzheimer beta-amyloid peptides mediated through specific binding to either phospholipids or gangliosides. Implications for neurotoxicity, J. Biol. Chem. 271 (1996) 26482–26489.
[6] R. Sultana, D.A. Butterfield, Alterations of some membrane transport proteins in Alzheimer's disease: role of amyloid beta-peptide, Mol. Biosyst. 4 (2008) 36–41.
[7] M. Hashimoto, S. Hossain, T. Shimada, O. Shido, Docosahexaenoic acid-induced protective effect against impaired learning in amyloid beta-infused rats is associated with increased synaptosomal membrane fluidity, Clin. Exp. Pharmacol. Physiol. 33 (2006) 934–939.
[8] E.A. Dennis, Diversity of group types, regulation, and function of phospholipase A2, J. Biol. Chem. 269 (1994) 13057–13060.
[9] J. Balsinde, M.A. Balboa, P.A. Insel, E.A. Dennis, Regulation and inhibition of phospholipase A2, Annu. Rev. Pharmacol. Toxicol. 39 (1999) 175–189.
[10] M. Murakami, I. Kudo, Phospholipase A2, J. Biochem. (Tokyo) 131 (2002) 285–292.
[11] A.A. Farooqui, L.A. Horrocks, Phospholipase A2-generated lipid mediators in the brain: the good, the bad, and the ugly, Neuroscientist 12 (2006) 245–260.

[12] O.V. Forlenza, E.L. Schaeffer, W.F. Gattaz, The role of phospholipase A2 in neuronal homeostasis and memory formation: implications for the pathogenesis of Alzheimer's disease, J. Neural. Transm. 114 (2007) 231–238.
[13] D. Stephenson, K. Rash, B. Smalstig, E. Roberts, E. Johnstone, J. Sharp, J. Panetta, S. Little, R. Kramer, J. Clemens, Cytosolic phospholipase A2 is induced in reactive glia following different forms of neurodegeneration, Glia 27 (1999) 110–128.
[14] A.A. Farooqui, W.Y. Ong, L.A. Horrocks, Plasmalogens, docosahexaenoic acid, and neurological disorders, in: F. Roels, M. Baes, S. de Bies (Eds.), Peroxisomal disorders and regulation of genes, Kluwer Academic/Plenum, London, 2003, pp. 335–354.
[15] A.A. Farooqui, W.Y. Ong, L.A. Horrocks, Stimulation of lipases and phospholipases in Alzheimer disease, in: B. Szuhaj, W. van Nieuwenhuyzen (Eds.), Nutrition and biochemistry of phospholipids, AOCS, Champaign, IL, 2003, pp. 14–29.
[16] J.R. Hibbeln, J.W. Palmer, J.M. Davis, Are disturbances in lipid–protein interactions by phospholipase-A2 a predisposing factor in affective illness? Biol. Psychiatry. 25 (1989) 945–961.
[17] D. Zhu, Y. Lai, P.B. Shelat, C. Hu, G.Y. Sun, J.C. Lee, Phospholipases A2 mediate amyloid-beta peptide-induced mitochondrial dysfunction, J. Neurosci. 26 (2006) 11111–11119.
[18] K.N. Dahlgren, A.M. Manelli, W.B. Stine Jr., L.K. Baker, G.A. Krafft, M.J. LaDu, Oligomeric and fibrillar species of amyloid-beta peptides differentially affect neuronal viability, J. Biol. Chem. 277 (2002) 32046–32053.
[19] J.P. Zhang, G.Y. Sun, Free fatty acids, neutral glycerides, and phosphoglycerides in transient focal cerebral ischemia, J. Neurochem. 64 (1995) 1688–1695.
[20] J.C. Lee, H. Bermudez, B.M. Discher, M.A. Sheehan, Y.Y. Won, F.S. Bates, D.E. Discher, Preparation, stability, and in vitro performance of vesicles made with diblock copolymers, Biotechnol. Bioeng. 73 (2001) 135–145.
[21] T. Parasassi, E. Gratton, W.M. Yu, P. Wilson, M. Levi, Two-photon fluorescence microscopy of laurdan generalized polarization domains in model and natural membranes, Biophys. J. 72 (1997) 2413–2429.
[22] T. Parasassi, M. Di Stefano, G. Ravagnan, O. Sapora, E. Gratton, Membrane aging during cell growth ascertained by Laurdan generalized polarization, Exp. Cell Res. 202 (1992) 432–439.
[23] J.C.-M. Lee, R.J. Law, D.E. Discher, Bending contributions hydration of phospholipid and block copolymer membranes: Unifying correlations between probe fluorescence and vesicle thermoelasticity, Langmuir 17 (2001) 3592–3597.
[24] D. Zhu, K.S. Tan, X. Zhang, A.Y. Sun, G.Y. Sun, J.C. Lee, Hydrogen peroxide alters membrane and cytoskeleton properties and increases intercellular connections in astrocytes, J. Cell. Sci. 118 (2005) 3695–3703.
[25] K.E. Chapman, S.E. Sinclair, D. Zhuang, A. Hassid, L.P. Desai, C.M. Waters, Cyclic mechanical strain increases reactive oxygen species production in pulmonary epithelial cells, Am. J. Physiol. Lung. Cell Mol. Physiol. 289 (2005) L834–841.
[26] M.M. Bradford, A rapid and sensitive method for the quantitation of microgram quantities of protein utilizing the principle of protein-dye binding, Anal. Biochem. 72 (1976) 248–254.
[27] T. Parasassi, G. De Stasio, A. d'Ubaldo, E. Gratton, Phase fluctuation in phospholipid membranes revealed by Laurdan fluorescence, Biophys. J. 57 (1990) 1179–1186.
[28] T. Parasassi, A.M. Giusti, E. Gratton, E. Monaco, M. Raimondi, G. Ravagnan, O. Sapora, Evidence for an increase in water concentration in bilayers after oxidative damage of phospholipids induced by ionizing radiation, Int. J. Radiat. Biol. 65 (1994) 329–334.
[29] T. Parasassi, G. Ravagnan, R.M. Rusch, E. Gratton, Modulation and dynamics of phase properties in phospholipid mixtures detected by Laurdan fluorescence, Photochem. Photobiol. 57 (1993) 403–410.
[30] S.A. Waschuk, E.A. Elton, A.A. Darabie, P.E. Fraser, J.A. McLaurin, Cellular membrane composition defines A beta-lipid interactions, J. Biol. Chem. 276 (2001) 33561–33568.
[31] J. Stolk, T.J. Hiltermann, J.H. Dijkman, A.J. Verhoeven, Characteristics of the inhibition of NADPH oxidase activation in neutrophils by apocynin, a methoxy-substituted catechol, Am. J. Respir. Cell Mol. Biol. 11 (1994) 95–102.
[32] G.P. Eckert, N.J. Cairns, A. Maras, W.F. Gattaz, W.E. Muller, Cholesterol modulates the membrane-disordering effects of beta-amyloid peptides in the hippocampus: specific changes in Alzheimer's disease, Dement. Geriatr. Cogn. Disord. 11 (2000) 181–186.
[33] A.Y. Abramov, J. Jacobson, F. Wientjes, J. Hothersall, L. Canevari, M.R. Duchen, Expression and modulation of an NADPH oxidase in mammalian astrocytes, J. Neurosci. 25 (2005) 9176–9184.
[34] K. Gaus, E. Gratton, E.P. Kable, A.S. Jones, I. Gelissen, L. Kritharides, W. Jessup, Visualizing lipid structure and raft domains in living cells with two-photon microscopy, Proc. Natl. Acad. Sci. U. S. A. 100 (2003) 15554–15559.
[35] C. Dietrich, L.A. Bagatolli, Z.N. Volovyk, N.L. Thompson, M. Levi, K. Jacobson, E. Gratton, Lipid rafts reconstituted in model membranes, Biophys. J. 80 (2001) 1417–1428.
[36] L.A. Bagatolli, E. Gratton, Two-photon fluorescence microscopy observation of shape changes at the phase transition in phospholipid giant unilamellar vesicles, Biophys. J. 77 (1999) 2090–2101.
[37] L.A. Bagatolli, E. Gratton, A correlation between lipid domain shape and binary phospholipid mixture composition in free standing bilayers: A two-photon fluorescence microscopy study, Biophys. J. 79 (2000) 434–447.
[38] D.L. Dinnes, J.P. Santerre, R.S. Labow, Intracellular phospholipase A2 expression and location in human macrophages: influence of synthetic material surface chemistry, J. Cell. Physiol. 214 (2008) 136–144.
[39] F.M. Harris, S.K. Smith, J.D. Bell, Physical properties of erythrocyte ghosts that determine susceptibility to secretory phospholipase A2, J. Biol. Chem. 276 (2001) 22722–22731.
[40] J.R. Dave, R.A. Knazek, S.C. Liu, Arachidonic acid, bradykinin and phospholipase A2 modify both prolactin binding capacity and fluidity of mouse hepatic membranes, Biochem. Biophys. Res. Commun. 103 (1981) 727–738.
[41] E.L. Schaeffer, F. Bassi Jr., W.F. Gattaz, Inhibition of phospholipase A2 activity reduces membrane fluidity in rat hippocampus, J. Neural. Transm. 112 (2005) 641–647.
[42] Y. Kameyama, S. Kudo, K. Ohki, Y. Nozawa, Differential inhibitory effects by phospholipase A2 on guanylate and adenylate cyclases of Tetrahymena plasma membranes, Jpn. J. Exp. Med. 52 (1982) 183–192.
[43] D.J. Selkoe, The ups and downs of Abeta, Nat. Med. 12 (2006) 758–759 discussion 759.
[44] M.P. Lambert, A.K. Barlow, B.A. Chromy, C. Edwards, R. Freed, M. Liosatos, T.E. Morgan, I. Rozovsky, B. Trommer, K.L. Viola, P. Wals, C. Zhang, C.E. Finch, G.A. Krafft, W.L. Klein, Diffusible, nonfibrillar ligands derived from Abeta1–42 are potent central nervous system neurotoxins, Proc. Natl. Acad. Sci. U. S. A. 95 (1998) 6448–6453.
[45] M.P. Mattson, B. Cheng, D. Davis, K. Bryant, I. Lieberburg, R.E. Rydel, beta-Amyloid peptides destabilize calcium homeostasis and render human cortical neurons vulnerable to excitotoxicity, J. Neurosci. 12 (1992) 376–389.
[46] A. Demuro, E. Mina, R. Kayed, S.C. Milton, I. Parker, C.G. Glabe, Calcium dysregulation and membrane disruption as a ubiquitous neurotoxic mechanism of soluble amyloid oligomers, J. Biol. Chem. 280 (2005) 17294–17300.
[47] W. Gibson Wood, G.P. Eckert, U. Igbavboa, W.E. Muller, Amyloid beta–protein interactions with membranes and cholesterol: causes or casualties of Alzheimer's disease, Biochim. Biophys. Acta. 1610 (2003) 281–290.
[48] W.E. Muller, G.P. Eckert, K. Scheuer, N.J. Cairns, A. Maras, W.F. Gattaz, Effects of beta–amyloid peptides on the fluidity of membranes from frontal and parietal lobes of human brain. High potencies of A beta 1–42 and A beta 1–43, Amyloid 5 (1998) 10–15.
[49] C.M. Yip, E.A. Elton, A.A. Darabie, M.R. Morrison, J. McLaurin, Cholesterol, a modulator of membrane-associated Abeta-fibrillogenesis and neurotoxicity, J. Mol. Biol. 311 (2001) 723–734.
[50] N.A. Avdulov, S.V. Chochina, U. Igbavboa, E.O. O'Hare, F. Schroeder, J.P. Cleary, W.G. Wood, Amyloid beta-peptides increase annular and bulk fluidity and induce lipid peroxidation in brain synaptic plasma membranes, J. Neurochem. 68 (1997) 2086–2091.
[51] S.V. Chochina, N.A. Avdulov, U. Igbavboa, J.P. Cleary, E.O. O'Hare, W.G. Wood, Amyloid beta-peptide1–40 increases neuronal membrane fluidity: role of cholesterol and brain region, J. Lipid. Res. 42 (2001) 1292–1297.
[52] J.J. Kremer, M.M. Pallitto, D.J. Sklansky, R.M. Murphy, Correlation of beta-amyloid aggregate size and hydrophobicity with decreased bilayer fluidity of model membranes, Biochemistry 39 (2000) 10309–10318.
[53] R.P. Mason, R.F. Jacob, M.F. Walter, P.E. Mason, N.A. Avdulov, S.V. Chochina, U. Igbavboa, W.G. Wood, Distribution and fluidizing action of soluble and aggregated amyloid beta-peptide in rat synaptic plasma membranes, J. Biol. Chem. 274 (1999) 18801–18807.
[54] A. Nunomura, G. Perry, G. Aliev, K. Hirai, A. Takeda, E.K. Balraj, P.K. Jones, H. Ghanbari, T. Wataya, S. Shimohama, S. Chiba, C.S. Atwood, R.B. Petersen, M.A. Smith, Oxidative damage is the earliest event in Alzheimer disease, J. Neuropathol. Exp. Neurol. 60 (2001) 759–767.
[55] A.Y. Abramov, L. Canevari, M.R. Duchen, Beta-amyloid peptides induce mitochondrial dysfunction and oxidative stress in astrocytes and death of neurons through activation of NADPH oxidase, J. Neurosci. 24 (2004) 565–575.
[56] Z. Shmelzer, N. Haddad, E. Admon, I. Pessach, T.L. Leto, Z. Eitan-Hazan, M. Hershfinkel, R. Levy, Unique targeting of cytosolic phospholipase A_2 to plasma membranes mediated by the NADPH oxidase in phagocytes, J. Cell. Biol. 162 (2003) 683–692.
[57] I. Hazan-Halevy, T. Levy, T. Wolak, I. Lubarsky, R. Levy, E. Paran, Stimulation of NADPH oxidase by angiotensin II in human neutrophils is mediated by ERK, p38 MAP-kinase and cytosolic phospholipase A_2, J. Hypertens. 23 (2005) 1183–1190.
[58] I. Pessach, T.L. Leto, H.L. Malech, R. Levy, Essential requirement of cytosolic phospholipase A_2 for stimulation of NADPH oxidase-associated diaphorase activity in granulocyte-like cells, J. Biol. Chem. 276 (2001) 33495–33503.
[59] R. Dana, T.L. Leto, H.L. Malech, R. Levy, Essential requirement of cytosolic phospholipase A_2 for activation of the phagocyte NADPH oxidase, J. Biol. Chem. 273 (1998) 441–445.
[60] R. Levy, A. Lowenthal, R. Dana, Cytosolic phospholipase A_2 is required for the activation of the NADPH oxidase associated H^+channel in phagocyte-like cells, Adv. Exp. Med. Biol. 479 (2000) 125–135.
[61] X. Zhao, E.A. Bey, F.B. Wientjes, M.K. Cathcart, Cytosolic phospholipase A_2 ($cPLA_2$) regulation of human monocyte NADPH oxidase activity. $cPLA_2$ affects translocation but not phosphorylation of $p67^{phox}$ and $p47^{phox}$, J. Biol. Chem. 277 (2002) 25385–25392.
[62] R. Levy, The role of cytosolic phospholipase A2-alfa in regulation of phagocytic functions, Biochim. Biophys. Acta. 1761 (2006) 1323–1334.
[63] E.H. Radany, M. Brenner, F. Besnard, V. Bigornia, J.M. Bishop, C.F. Deschepper, Directed establishment of rat brain cell lines with the phenotypic characteristics of type 1 astrocytes, Proc. Natl. Acad. Sci. U. S. A. 89 (1992) 6467–6471.
[64] C.M. Yip, A.A. Darabie, J. McLaurin, Abeta42-peptide assembly on lipid bilayers, J. Mol. Biol. 318 (2002) 97–107.
[65] H.A. Wilson, W. Huang, J.B. Waldrip, A.M. Judd, L.P. Vernon, J.D. Bell, Mechanisms by which thionin induces susceptibility of S49 cell membranes to extracellular phospholipase A2, Biochim. Biophys. Acta. 1349 (1997) 142–156.
[66] J. Janson, R.H. Ashley, D. Harrison, S. McIntyre, P.C. Butler, The mechanism of islet amyloid polypeptide toxicity is membrane disruption by intermediate-sized toxic amyloid particles, Diabetes 48 (1999) 491–498.
[67] S. Janciauskiene, B. Ahren, Fibrillar islet amyloid polypeptide differentially affects oxidative mechanisms and lipoprotein uptake in correlation with cytotoxicity in two insulin-producing cell lines, Biochem. Biophys. Res. Commun. 267 (2000) 619–625.